

The correlation line of the His117Gly type-2 proteins runs below the line of the other type-2 copper centers in Figure 7. This can be attributed to the presence of the sulfur in the Cu coordination shell in the His117Gly type-2 proteins.^{37,38} The smaller values of the g_{\parallel} of His117Gly(His) and -(Hista) compared to those of His117Gly(H₂O) and -(ImAc) may reflect the aromaticity of the His and Hista ligands and the replacement of the less electron-rich oxygens of one or two water molecules or of the carbonyl of ImAc by one or two coordinating more electron-rich nitrogens.³⁷

In the case of His117Gly(H₂O), one or two hydroxide ions could coordinate instead of water molecules. However, this seems less likely because the change in g_{\parallel} upon incubation of His117Gly-(H₂O) by His is much larger than expected for a replacement of OH⁻ by His.³⁵

Concluding Remarks

The replacement of the His117 ligand of azurin by a glycine apparently does not change the structure of the protein noticeably or the pocket which contains the copper ion. However, the important contribution of His117 to the biological function of azurin is best illustrated by the observation that the His117Gly(L) species that cluster around B in Figure 6 behave spectroscopically virtually identical to the wild type but are not functional in reversible electron transfer.

Geometrical changes of the copper center could be induced by various exogenous ligands and cause this one mutant to spectroscopically encompass the known range of type-1 and part of the range of the type-2 copper proteins. An interesting observation is that the His117Gly points in Figure 6 are not scattered more or less evenly along the correlation line connecting regions A and C but cluster in three areas. We tentatively interpret this as indicating a preference by the protein for a few discrete adaptations around the Cu site instead of a continuous variation.

In conclusion, it is interesting to note that a large variety of external ligands appear compatible with a metal center that retains the basic features of a type-1 or type-2 Cu site. It opens the attractive possibility of obtaining deeper insight into the correlation between copper site geometry and spectroscopic and mechanistic features by means of further detailed structural studies.

Acknowledgment. The authors thank Drs. S. J. P. Albracht for recording the S- and Q-band EPR spectra and A. C. F. Gorren for assisting with the stopped-flow measurements. They thank Prof. E. I. Solomon for valuable comments. For stimulating discussions they thank Profs. J. Reedijk, J. Sanders-Loehr, and T. M. Loehr and Drs. C. W. G. Houtink and M. Ubbink. This research was supported by the Technology Foundation (STW), which is subsidized by the Department of Economic Affairs.

Tetrafluorosulfate(1-) and Tetrafluorooxosulfate(1-) Radical Anions (SF₄⁻ and SF₄O⁻)^{†,‡}

K. O. Christe,^{*4} D. A. Dixon,³ I. B. Goldberg,² C. J. Schack,⁴ B. W. Walther,^{1,§} J. T. Wang,¹ and F. Williams^{*1}

Contribution from the Department of Chemistry, University of Tennessee, Knoxville, Tennessee 37996-1600, Science Center, Rockwell International Corporation, Thousand Oaks, California 91360, Central Research Department, Experimental Station, E.I. DuPont de Nemours and Company, Wilmington, Delaware 19880-0328, and Rocketdyne Division, Rockwell International, Canoga Park, California 91309-7922. Received August 10, 1992

Abstract: The novel radical anions SF₄⁻ and *trans*-SF₄O⁻ were generated by γ -irradiation of CsSF₅ and CsSF₅O, respectively, at -196 °C and characterized by their isotropic EPR spectra at +27 °C. The SF₄⁻ anion ($g = 2.0045$, $a_{33S} = 12.85$ mT, $a_{19F} = 9.75$ mT) has a square-planar structure close to D_{4h} symmetry derived from a pseudo-octahedron in which the two axial positions are equally occupied by a total of three sterically active valence electrons. Accordingly, the greatest portion of the unpaired electron spin is localized in a sulfur p_z orbital. The *trans*-SF₄O⁻ anion ($g = 2.0027$, $a_{33S} = 36.26$ mT, $a_{19F} = 18.95$ mT) has a closely related, pseudo-octahedral structure of C_{4v} symmetry in which the equatorial positions are occupied by four equivalent fluorines, one axial position is occupied by a doubly bonded oxygen, and the second axial position is occupied by the sterically active free valence electron. Accordingly, the greatest portion of the unpaired electron spin is localized in an axial sp-hybrid orbital of sulfur. The structures and electron spin density distributions of SF₄⁻ and *cis*- and *trans*-SF₄O⁻ were analyzed by a local density functional study which also provided vibrational frequencies and charge distributions for these radical anions. For comparison, the closely related SF₅ radical, the *cis*- and *trans*-PF₄O²⁻ radical anions, and the SF₄, SF₄O, and SF₆ molecules were also calculated by this method. These calculations show that the exclusive formation of *trans*-SF₄O⁻ under our experimental conditions is probably due to both energetic and reaction mechanistic reasons and that the agreement between the LDF calculations and the experimental data is good.

Introduction

Previous studies have demonstrated that γ -irradiation of salts containing complex fluoro ions can result in the loss of one fluorine atom and in the formation of new complex fluoro radical ions that contain one fluorine atom less than the parent ion. Thus, the

radical ions PF₅⁻⁵⁻⁸, AsF₅^{-8,9} and NF₃^{+10,11} have been obtained from PF₆⁻, AsF₆⁻, and NF₄⁺ containing salts, respectively, and

[†] Dedicated to Professor Felix Aubke on the occasion of his 60th birthday.

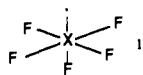
[‡] Based in part on the PhD. dissertation of B. W. Walther, University of Tennessee, 1984. A preliminary report of this work was presented at the 186th ACS National Meeting, Washington, D.C., August 28-September 2, 1983; Abstract FLUO 31.

[§] Present address: Dow Chemical Co., Louisiana Research & Development, P.O. Box 400, Plaquemine, LA 70765-0400.

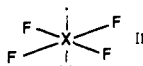
- (1) University of Tennessee.
- (2) The Science Center, Rockwell International Corp.
- (3) E.I. DuPont de Nemours and Co.
- (4) The Rocketdyne Division, Rockwell International Corp.
- (5) (a) Morton, J. R. *Can. J. Phys.* **1963**, *41*, 706. (b) Atkins, P. W.; Symons, M. C. R. *J. Chem. Soc.* **1964**, 4363.
- (6) Morton, J. R.; Preston, K. F. In *Fluorine-Containing Free Radicals*; Root, J. W., Ed.; ACS Symposium Series 66, American Chemical Society: Washington, D.C., 1978; p 386.
- (7) Mishra, S. P.; Symons, M. C. R. *J. Chem. Soc., Chem. Commun.* **1974**, 279.

characterized by electron paramagnetic resonance (EPR) spectroscopy.

Characterization by EPR is not always unambiguous. For example, the pseudo-octahedral XF_5 radicals PF_5^{-7} and SF_5^{12}



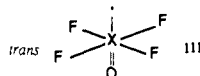
exhibited detectable hyperfine splittings (hfs) only for the four equatorial fluorine atoms but, surprisingly, not for the axial fluorine atom. For PF_5 this led originally to an incorrect identification as PF_4 .⁵ In this respect, it seemed interesting to prepare the yet unknown SF_4^- radical. By comparison with the known isoelectronic ClF_4 radical,¹³⁻¹⁵ a pseudo-octahedral structure with a square-planar XF_4 moiety



can be expected for SF_4^- . Therefore, the EPR spectrum of SF_4^- should, in general appearance, resemble that of the SF_5 radical,¹² but the g -factor and ^{19}F and ^{33}S hyperfine splittings should be significantly different.

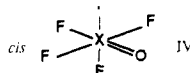
After completion of this work, the results of a theoretical investigation on the molecular and electronic structure of the SF_n ($n = 1-5$) and their singly charged negative ions using density functional theory was published which also predicted an approximately square-planar structure for SF_4^- .¹⁶

Similarly, the preparation of the yet unknown SF_4O^- radical anion should be interesting. Its structure is expected to be similar to that of SF_4^- , except for the replacement of the axial free valence electron pair by an oxygen ligand.



Since ^{16}O does not possess a nuclear spin, the EPR pattern of SF_4O^- should again resemble those of SF_5 and SF_4^- in general appearance, but with a different g -factor and hyperfine splittings.

For SF_4O^- , additional interest comes from the fact that the isoelectronic PF_4O^{2-} and $\text{AsF}_4\text{O}^{2-}$ radical anions⁸ exhibit two stereoisomers (III and IV). Isomer III, labeled trans, has one axial oxygen ligand opposite to the orbital containing the unpaired electron. Isomer IV has one equatorial oxygen ligand adjacent to the orbital containing the unpaired electron. It would be interesting to examine whether such isomerism is also observable for SF_4O^- .



Experimental Section

The samples of CsSF_5 and CsSF_5O were prepared as previously described,^{17,18} from dry CsF and SF_4 or SF_4O . On the basis of the observed

(8) Morton, J. R.; Preston, K. F.; Strach, S. J. *J. Magn. Reson.* **1980**, *37*, 321.

(9) Symons, M. C. R. *Int. J. Radiat. Phys. Chem.* **1976**, *8*, 643.

(10) Mishra, S. P.; Symons, M. C. R.; Christe, K. O.; Wilson, R. D.; Wagner, R. I. *Inorg. Chem.* **1975**, *14*, 1103.

(11) Goldberg, I. B.; Crowe, H. R.; Christe, K. O. *Inorg. Chem.* **1978**, *17*, 3189.

(12) (a) Morton, J. R.; Preston, K. F. *Chem. Phys. Lett.* **1973**, *18*, 98. (b) Hasegawa, A.; Williams, F. *Chem. Phys. Lett.* **1977**, *45*, 275.

(13) (a) Morton, J. R.; Preston, K. F. *J. Chem. Phys.* **1973**, *58*, 3112. (b) Nishikida, K.; Williams, F.; Mamantov, G.; Smyrl, N. *J. Am. Chem. Soc.* **1975**, *97*, 3526.

(14) Gregory, A. R. *J. Chem. Phys.* **1974**, *60*, 3713.

(15) (a) Ungemach, S. R.; Schaefer, H. F. *J. Am. Chem. Soc.* **1976**, *98*, 1658. (b) So, S. P.; Richards, W. G. *J. Chem. Soc., Faraday Trans. II* **1979**, *75*, 55.

(16) Ziegler, T.; Gutsev, G. L. *J. Chem. Phys.* **1992**, *96*, 7623.

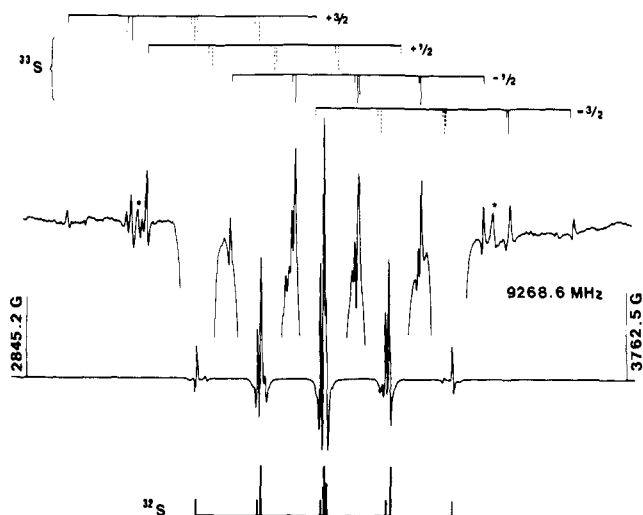


Figure 1. EPR spectrum and spectral analysis of the SF_4^- anion radical. The upper trace was obtained by signal averaging from 30 scans and recorded at 500 times the gain of the lower trace. The lines marked by an asterisk do not belong to the pattern of SF_4^- .

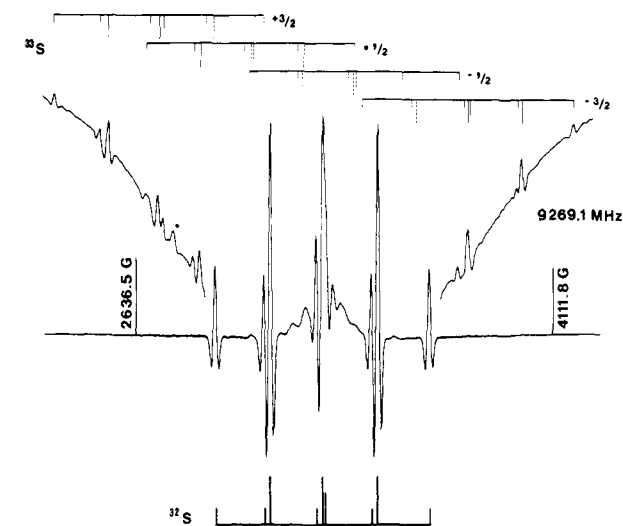


Figure 2. EPR spectrum and spectral analysis of the SF_4O^- anion radical. The upper trace was obtained by signal averaging from 30 scans and recorded at 500 times the gain of the lower trace. The line marked by an asterisk does not belong to the pattern of SF_4O^- .

material balances, the conversion of CsF was 50% for CsSF_5 and 85% for CsSF_5O . The purity of the compounds was verified by Raman spectroscopy, which showed only the bands characteristic^{17,18} of SF_5^- and SF_5O^- , respectively. In the dry nitrogen atmosphere of a glovebox, the samples were loaded into flame-out 4-mm o.d. Suprasil EPR sample tubes (Wilma Glass Co.) that were flame-sealed under vacuum. These tubes were then irradiated in a ^{60}Co γ -radiation source (Gammacel 200, Nordion International, Inc., Kanata, Ontario, Canada) at a dose rate of 1.03×10^5 rad/h for a total dose of 4 Mrad (4×10^4 J/kg). The EPR spectra were recorded at sample temperatures ranging from -190 to 90°C . Since the spectral features did not sharpen up any further above room temperature and a slight amount of decay was observed above 60°C , the reported spectra were recorded at ambient temperature. Preliminary work with a Varian V4302-15 EPR spectrometer led to the detection of the main ^{32}S spectra of the subject radicals while the ^{33}S satellite lines in natural abundances were only revealed by optimization of microwave power (4 dB \approx 79 mW) and modulation amplitude (1.25–2.5 mT) using a more sensitive Bruker ER 200D SRC instrument.

Computations were carried out in the local density functional (LDF) approximation¹⁹ by using the program system DMol,^{20,21} as previously

(17) Christe, K. O.; Curtis, E. C.; Schack, C. J.; Pilipovich, D. *Inorg. Chem.* **1972**, *11*, 1679.

(18) Christe, K. O.; Schack, C. J.; Pilipovich, D.; Curtis, E. C.; Sawodny, W. *Inorg. Chem.* **1973**, *12*, 620.

Table I. Hyperfine Splittings, *g*-Factors, and *s*-Orbital Electron Spin Densities of SF₄⁻ and SF₄O⁻ and Related Radicals Calculated from the Observed Hyperfine Splittings

radical	<i>a</i> _X (mT)	<i>n</i> _F ^b	<i>a</i> _F (mT)	<i>g</i> -factor	$\rho_s^{X,c}$	$\rho_s^{F,c}$	ref
³³ SF ₄ ⁻	12.85	4	9.75	2.0045	0.104	0.0052	a
³⁵ ClF ₄	28.82	4	7.87	2.0117	0.141	0.0042	13
³³ SF ₄ O ⁻	36.26	4	18.95	2.00274	0.293	0.0105	a
³³ SF ₃	30.68	4	14.30	2.0044	0.248	0.0076	12, 23, 24a
⁷⁵ SeF ₅	187.7	4	11.80	2.0072	0.261	0.0063	24a
³¹ PF ₅ ⁻	135.6	4	19.8	2.0017	0.286	0.0105	7, 8
			0.3			0.0002	
⁷⁵ AsF ₅ ⁻	182.9	4	18.3	1.9996	0.350	0.0097	8
			0.5			0.0003	
³¹ PF ₄ O ²⁻							8
trans	139.0	4	21.2	2.0019	0.293	0.0112	
cis ^d	124.3	2	22.4	2.0025	0.261	0.0119	
		1	17.6			0.0093	
⁷⁵ AsF ₄ O ²⁻							8
trans	185.0	4	19.3	1.9998	0.354	0.0102	
cis ^d	165.1	2	21.9	2.0011	0.316	0.0116	
		1	15.4			0.0082	

^aThis work. ^bNumber of equivalent fluorine atoms. ^cCalculated based on parameters given in ref 24b. ^dNo splittings due to interactions with the apical fluorine ligand were observed.

described in more detail.²²

The SCF equations for the triplet states were solved by spin unrestricted methods similar to those employed in unrestricted Hartree-Fock (UHF) calculations. Geometries were optimized by using analytic gradient methods.²¹ There are two problems with evaluating gradients in the LDF framework which are due to the numerical methods that are used. The first is that the energy minimum does not necessarily correspond exactly to the point with a zero derivative. The second is that the sum of the gradients may not always be zero, as required for translational invariance. These tend to introduce errors on the order of 0.001 Å in the calculation of the coordinates if both a reasonable grid and basis set are used. This gives bond lengths and angles with reasonable error limits. The difference of 0.001 Å is about an order of magnitude smaller than the accuracy of the LDF geometries as compared to experiment. The frequencies were determined by numerical differentiation of the gradient. A two-point difference formula was used with a displacement of 0.01 au.

Results and Discussion

EPR Spectra. The second-derivative isotropic EPR spectra of the SF₄⁻ and SF₄O⁻ radical ions are shown in Figures 1 and 2, respectively. Each spectrum shows the satellite lines due to naturally abundant ³³S. At sample temperatures from -50 to 90 °C, the spectra gave only slight indications of residual anisotropy, suggesting that, in this range, the radicals rotate freely at their lattice positions. Because the hyperfine splittings are large, the azimuthal nuclear spin quantum number, *M*_l, lines for ¹⁹F exhibit "second-order" splittings^{23,24} and the *M*_l lines for ³³S exhibit shifts, making the separation between lines nonlinear in *M*_l. The analyses of the spectra of the ³²S-centered radicals, including the higher

(19) (a) Parr, R. G.; Yang, W. *Density Functional Theory of Atoms and Molecules*; Oxford University Press: New York, 1989. (b) Salahub, D. R. In *Ab Initio Methods in Quantum Chemistry*; Lawley, K. P., Ed.; J. Wiley & Sons: New York, 1987; Vol. II, p 447. (c) Wimmer, E.; Freeman, A. J.; Fu, C.-L.; Cao, P.-L.; Chou, S.-H.; Delley, B. In *Supercomputer Research in Chemistry and Chemical Engineering*; Jensen, K. F., Truhlar, D. G., Eds.; ACS Symposium Series, American Chemical Society: Washington, D.C., 1987; p 49. (d) Jones, R. O.; Gunnarsson, O. *Rev. Mod. Phys.* **1989**, *61*, 689. (e) Zeigler, T. *Chem. Rev.* **1991**, *91*, 651. (f) Dixon, D. A.; Andzelm, A.; Fitzgerald, G.; Wimmer, E.; Delley, B. In *Science and Engineering on Supercomputers*; Pitcher, E. J., Ed.; Computational Science Publications: Southampton, England, 1990; p 285. (g) Dixon, D. A.; Andzelm, J.; Fitzgerald, G.; Wimmer, E.; Jasien, P. In *Density Functional Methods in Chemistry*; Labanowski, J., Andzelm, J., Eds.; Springer-Verlag: New York, 1991; p 33.

(20) Delley, B. *J. Chem. Phys.* **1990**, *92*, 508. DMol is available commercially from BIOSYM Technologies, San Diego, CA.

(21) Delley, B. In *Density Functional Methods in Chemistry*; Labanowski, J., Andzelm, J., Eds.; Springer-Verlag: New York, 1991; p 101.

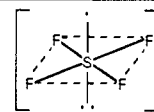
(22) Christie, K. O.; Curtis, E. C.; Dixon, D. A.; Mercier, H. P.; Sanders, J. C. P.; Schrobilgen, G. J. *J. Am. Chem. Soc.* **1991**, *113*, 3351.

(23) Fessenden, R. W. *J. Magn. Reson.* **1969**, *1*, 277.

(24) (a) Morton, J. R.; Preston, K. F.; Tait, J. C. *J. Chem. Phys.* **1975**, *62*, 2029. (b) Morton, J. R.; Preston, K. F. *J. Magn. Reson.* **1978**, *30*, 577.

Table II. Geometry, Unscaled Vibrational Spectrum, Spin Populations, and Atomic Charges Calculated for SF₄⁻ by the LDF Method

Geometry	C _{4v}	D _{4h}
r S-F (Å)	1.793	1.803
∠ FSF (deg)	89.2	90
∠ FS-C _{4v} axis (deg)	83.3	90
Vibrational Frequencies (cm ⁻¹)		
approx. mode description		
v sym SF ₄ in phase	A ₁ v ₁ 547	A _{1g} v ₁ 516
δ sym SF ₄ out of plane, in ph.	v ₂ 299	A _{1u} v ₂ 245i
v sym SF ₄ out of phase	B ₁ v ₃ 425	B _{1g} v ₃ 406
δ sym SF ₄ out of plane, out of ph.	v ₄ 130	B _{1u} v ₄ 121
δ sciss SF ₄	B ₂ v ₅ 274	B _{2g} v ₅ 258
v as SF ₄	E v ₆ 612	E _u v ₆ 604
δ as SF ₄ in plane	v ₇ 227	v ₇ 210
Spin Populations		
atom orbital		
S 3s	0.033	-0.014
S 3px,y } 3p	0.013	
S 3pz } 3p	0.602	0.627
S 3dxy,x ² -y ² } 3d	0.001	
S 3dxz,yz } 3d	0.003	0.026
S 3dz ² } 3d	0.019	0.021
F 2px,y } 2p	0.016	
F 2pz } 2p	0.045	0.078
Atomic Charges		
S		0.725
F		-0.431

**Table III.** Geometries, Unscaled Vibrational Spectra, Spin Populations, and Atomic Charges Calculated for the *trans*-PF₄O²⁻, SF₄O⁻, and SF₃ Radicals and the Observed Vibrational Spectrum of ClF₄O⁻

Geometry	C _{4v}	C _{2v}	C _{4v}	C _{4v}
r X-Y (Å)	1.530	1.464		1.587
r X-F (Å)	1.841	1.770		1.645
∠ YXF (deg)	100.3	101.6		91.7
Vibrational Frequencies (cm ⁻¹)				
approx. mode description				
A ₁ v ₁ vX-Y	1096	1211	1203	837
v ₂ v sym XF ₄	422	503	456	605
v ₃ δ sym in phase XF ₄ out of plane	354	361	339	461
B ₁ v ₄ sym XF ₄ out of phase	333	421	345	563
v ₅ δ sym out of phase XF ₄ out of plane	159	148	283	201
B ₂ v ₆ δ sciss XF ₄	267	315	243	403
E v ₇ v as XF ₄	538	635	578	809
v ₈ δ YXF ₄	329	375	406	453
v ₉ δ as XF ₄ in plane	203	250	204	311
Spin Populations				
atom ^a orbital				
X 3s	0.412	0.258		0.258
X 3px,y } 3p	0.227	0.239	0.169	0.201
X 3pz } 3p	0.001	-0.002		0.075
X 3dxy,x ² -y ² } 3d	0.039	0.002	0.027	
X 3dxz,yz } 3d	0.030	0.024		0.069
F 3s	-0.004	-0.002		-0.001
F 2px,y } 2p	0.007	0.067		0.046
F 2pz } 2p	0.002	0.004	0.136	0.026
Y 2s	-0.005	-0.003		-0.004
Y 2px,y } 2p	0.027	-0.005	0.016	-0.001
Y 2pz } 2p		0.025		-0.002
Atomic Charges				
X	0.610	0.864		0.996
F	-0.504	-0.376		-0.212
Y	-0.593	-0.360		-0.148

^aX = P, S, or Cl; Y = O or the unique F.

order effects for the fluorine hyperfine lines, are given below the spectra, and those for the ³³S-centered radicals are given above the spectra. The EPR parameters were determined using a least-squares matrix diagonalization program,²⁵ and the isotropic hyperfine splittings and *g*-factors of these radicals and other analogous species^{7,8,12,13,23,24} are given in Table I. Spin densities in the *s* orbitals of the central atoms or fluorine, X, were calculated according to

$$\rho_s^X = a_X / a_X^0$$

(25) Hasegawa, A.; Hayashi, M.; Kerr, C. M. L.; Williams, F. J. *Magn. Reson.* **1982**, *48*, 192.

where a_X and a_X° are respectively the isotropic hyperfine splitting of atom X in the radical and the hyperfine splitting of the atom assuming that there was one unpaired electron in the outermost s orbital of that atom.²⁵

EPR spectra showing varying degrees of ¹⁹F hyperfine anisotropy were obtained in each case with sample temperatures below -50 °C. In particular, the spectrum of SF₄⁻ between -190 and -170 °C consisted of a strong central absorption at $g = 2.005$ flanked by three pairs of broad features separated by ca. 40.0, 47.0, and 55.0 mT. The two outer pairs of wing features must be anisotropic components, since the total width of the ³²SF₄⁻ anisotropic spectrum is only 29.0 mT. Between -170 and -80 °C, these outer features gradually weakened while an additional pair of lines, separated by ca. 20 mT and destined to become the $M_1 = \pm 1$ lines of the isotropic spectrum at higher temperatures, developed considerable intensity. The low-temperature spectra of SF₄O⁻ recorded below -70 °C revealed a pair of anisotropic features, separated by ca. 90.1 mT, in addition to broad resonances at the isotropic positions, but otherwise the spectra were not very informative in this low-temperature region.

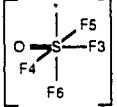
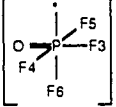
Local Density Functional Calculations. The geometries, vibrational spectra, spin populations, and atomic charges for the SF₄⁻, *cis*- and *trans*-SF₄O⁻, *cis*- and *trans*-PF₄O²⁻, and SF₅ radicals were calculated using local density functional theory. The results are summarized in Tables II-IV.

For SF₄⁻, a C_{4v} structure, which deviates from the planar configuration by 6.7° and has an FSF bond angle of 89.2°, was found to be the energy minimum on the potential energy surface, in excellent agreement with the results from an independent LDF calculation.¹⁶ The planar D_{4h} structure is 1.51 kcal mol⁻¹ higher in energy and is a transition state characterized by an imaginary frequency (ν_2 in Table II). Since the axial positions in SF₄⁻ are occupied by free valence electrons which can rapidly move from one side of the SF₄ plane to the other, thereby creating the possibility for inversion, the potential energy curve of the C_{4v} model of SF₄⁻ has two minima, one at 6.7° above and one at 6.7° below the plane. The planar D_{4h} structure represents the inversion barrier, and the energy difference of 1.51 kcal mol⁻¹ between the C_{4v} and the D_{4h} structures is the barrier height. The inversion mode is the symmetric out of plane deformation, $\nu_2(A_1)$, with a zero-point energy of one half of 299 cm⁻¹ or 0.43 kcal mol⁻¹. In view of the small energy required for inversion, the assumption of a D_{4h} ground-state symmetry for SF₄⁻ under normal conditions is not unreasonable. As can be seen from Table II, the properties of SF₄⁻ do not change much between the C_{4v} and the D_{4h} configurations. As expected, the largest change involves the inversion mode, i.e. the symmetric out of plane deformation mode, ν_2 .

For SF₄O⁻ and isoelectronic PF₄O²⁻, the lowest energy structures are configuration III of symmetry C_{4v} (see Introduction), in which the sterically active unpaired electron is trans to the oxygen ligand. According to our calculations, the *trans* isomers of SF₄O⁻ and PF₄O²⁻ are 8.6 and 5.6 kcal mol⁻¹, respectively, lower in energy than their *cis* isomers (IV), and both isomers are minima on the potential energy surfaces. The exclusive formation of *trans*-SF₄O⁻ in our study is favored from energetic considerations. From reaction mechanistic arguments both isomers are about equally favored. Although the exact lengths of the axial and the equatorial fluorine bonds in SOF₅⁻ are unknown,^{26a} those in closely related TeOF₅⁻ and IOF₅^{26b} are about equal. Therefore, breakage of either fluorine bond should be about equally likely. In the previous study on PF₄O²⁻, in which both isomers were observed,⁸ these radical anions were generated from unidentified hydrolysis products of PF₆⁻ and, therefore, may have involved intramolecular HF elimination from hydroxy-substituted phosphorus fluoride anions. Since such an HF elimination would involve neighboring *cis* ligands, the formation of some *cis*-PF₄O²⁻ could be readily explained.

The fact that, in the *trans*-XF₄O radical anions, the F-X-O angles are about 101° and are significantly larger than 90° demonstrates that a doubly bonded oxygen ligand is more repulsive than a sterically active unpaired valence electron. As expected, a singly bonded fluorine ligand is much less repulsive than a doubly

Table IV. Calculated Geometries, Unscaled Vibrational Spectra, Spin Populations, and Atomic Charges for the *cis*-SF₄O⁻ and *cis*-PF₄O²⁻ Radical Anions

		C _s		C _s			
							
Geometry							
rX-O (Å)		1.490		1.558			
rX-F3		1.860		1.945			
rX-F4, rX-F5		1.753		1.822			
rX-F6		1.656		1.704			
∠ F3-X-O (deg)		169.0		174.1			
∠ F4-X-O		96.0		96.8			
∠ F6-X-O		103.1		101.1			
∠ F4-X-F6		88.2		88.7			
∠ F4-X-F5		168.0		166.5			
∠ F3-X-F4		84.2		83.3			
∠ F3-X-F6		87.9		84.8			
Spin Populations ^a							
atom	orbital						
X	3s	0.238		0.387			
X	3py	0.042		0.055			
X	3pz	0.082	} 0.131	0.078	} 0.211		
X	3px	0.007		0.078			
X	3dxy			0.008			
X	3dyz			0.008			
X	3dz ²	0.010	} 0.046	0.008	} 0.068		
X	3dxz	0.029		0.028			
X	3dx ² -y ²	0.007		0.016			
O	2s	0.002		-0.004			
O	2py	0.106		0.080			
O	2pz	0.070	} 0.182	0.028	} 0.136		
O	2px	0.004		0.028			
F3	2s			-0.002			
F3	2py	0.215		0.103			
F3	2pz	0.011	} 0.227	0.004	} 0.110		
F3	2px			0.004			
F4	2s	-0.001		-0.004			
F4	2pz	-0.001		0.007			
F4	2px	0.086	} 0.085	0.044	} 0.050		
F5	2s	-0.001				-0.004	
F5	2pz	0.086		0.044			
F5	2px	-0.001	} 0.085	0.007	} 0.050		
F6	2s	-0.003				-0.005	
F6	2pz	0.013		0.003			
F6	2px	0.001	} 0.013	0.003	} 0.005		
Vibrational Frequencies (cm ⁻¹)							
		1101		991			
		708		655			
		644		545			
		498		434			
		451		405			
		427		366			
		399		334			
		367		316			
		318		279			
		283		242			
		270		239			
		158		152			
Atomic charges							
X		0.80		0.54			
O		-0.37		-0.59			
F3		-0.41		-0.55			
F4		-0.37		-0.49			
F5		-0.37		-0.49			
F6		-0.28		-0.41			

^a The X-O axis is approximately the y axis, and F4, F5, and F6 are approximately in the x,z plane.

bonded oxygen but still slightly more so than an unpaired valence electron. This is shown by the F_{ax}-S-F_{eq} bond angle of 91.7° calculated for the SF₅ radical (see Table III).

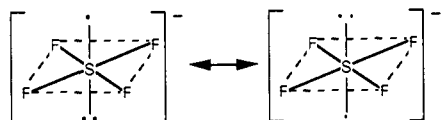
Since no experimental geometries nor vibrational frequencies are known for these radicals, with the exception of two infrared bands attributed²⁷ to SF₅ in a matrix, it was important to test the accuracy of our LDF calculations for closely related, well-known molecules. For this purpose, the geometries and vibrational spectra of SF₄,²⁸⁻³² SF₄O,^{29,30,33-36} and SF₆^{37,38} were calculated by the LDF method and, in Table V, are compared to the experimental data. As can be seen from this table, LDF theory duplicates well the observed geometries and vibrational frequencies, particularly if it is kept in mind that, for these types of fluorides,²² LDF theory generally predicts bond lengths which are about 0.04-Å longer than the observed ones. Therefore, the values calculated for the radicals of this study are also deemed to be good approximations to the true values, particularly if the calculated bond lengths are corrected (shortened) by about 0.04 Å. Of the two infrared bands previously reported for SF₅ in an Ar matrix,²⁷ the very intense

Table V. Calculated and Experimental Geometries and Unscaled Vibrational Spectra of SF₄, SF₄O, and SF₆

Geometry	C _{2v}		C _{2v}		C _h			
	calcd	obsd [29,31]	calcd	obsd [29,33,34,36]	calcd	obsd [37,38]		
r S-F ax (Å)	1.679	1.646	1.628	1.593	1.593	1.564		
r S-F eq	1.607	1.545	1.590	1.535				
r S-O	—	—	1.437	1.406				
∠ F _{ax} -S-F _{ax} (deg)	172.9	173.1	163.3	164.4	180	180		
∠ F _{eq} -S-F _{eq}	100.6	101.6	112.3	114.9	90	90		
Vibrational Frequencies (cm ⁻¹)								
A ₁ v ₁	826	892	A ₁ v ₁	1340	1380	A _{1g} v ₁	713	774
v ₂	560	558	v ₂	730	796	E _g v ₂	627	642
v ₃	453	532	v ₃	582	588	F _{1u} v ₃	934	948
v ₄	193	228	v ₄	511	566	v ₄	556	616
A ₂ v ₅	402	[437]	v ₅	136	174	F _{2g} v ₅	472	525
B ₁ v ₆	811	867	A ₂ v ₆	505	—	F _{2u} v ₆	309	347
v ₇	305	353	B ₁ v ₇	870	924			
B ₂ v ₈	782	730	v ₈	508	566			
v ₉	464	475	v ₉	232	265			
			B ₂ v ₁₀	837	815			
			v ₁₁	574	640			
			v ₁₂	497	447			

one at 812 cm⁻¹ is in excellent agreement with our calculated value of 809 cm⁻¹ for ν₇(E), but the frequency of the weak band observed at 552 cm⁻¹ appears somewhat high when compared to the value of 453 cm⁻¹ calculated for ν₇(E). This raises a question as to whether the 552-cm⁻¹ band belongs to SF₃.

SF₄⁻ Radical Anion. The paramagnetic species generated by γ-irradiation of Cs⁺SF₅⁻ is attributed to the novel SF₄⁻ radical anion for the following reasons. Its EPR spectrum shows the presence of four equivalent nuclei with spin *I* = 1/2 attributed to ¹⁹F, and the satellite lines reveal the presence of a nucleus of spin *I* = 3/2 at the 0.2% intensity expected for naturally abundant ³³S. Furthermore, the *s*-orbital spin densities on sulfur, ρ_s, and on fluorine, ρ_f, derived from the hyperfine splittings, and the *g*-factor are similar to those of the known,¹³ isoelectronic ClF₄ radical (see Table I). As shown by the LDF calculations for SF₄⁻ (see Table II) and the CNDO and INDO calculations for ClF₄,¹⁴ the most stable geometry for these two XF₄ radicals is a near-square-planar structure of approximate D_{4h} symmetry in which the electron densities above and below the plane are about equal, as depicted by the two mesomeric structures.

The small C_{4v} distortions, suggested for SF₄⁻ and ClF₄ by the LDF

(26) (a) Although the crystal structure of (Me₂N)₃S⁺SF₅O⁻ has recently been published (Heilemann, W.; Mews, R.; Pohl, S.; Saak, W. *Chem. Ber.* **1989**, *122*, 427), no reliable individual bond lengths were obtained for SF₅O⁻ due to disorder of the anion. (b) In TeOF₅, the axial and the equatorial fluorine bonds are of almost equal length (see: Miller, P. K.; Abney, K. D.; Rappé, A. K.; Anderson, O. P.; Strauss, S. H. *Inorg. Chem.* **1988**, *27*, 2255), and a recent study of IOF₃ (Christe, K. O.; Curtis, E. C.; Dixon, D. A. *J. Fluorine Chem.*, in press) has shown that the same applies to this molecule and that the previously reported (Bartell, L. S.; Clippard, F. B.; Jacob, E. J. *Inorg. Chem.* **1976**, *15*, 3009) structure should be revised.

(27) Smardzewski, R. R.; Fox, W. B. *J. Chem. Phys.* **1977**, *67*, 2309.

(28) Sawodny, W.; Birk, K.; Fogarasi, G.; Christe, K. O. *Z. Naturforsch.*, **B** **1980**, *35B*, 1137.

(29) Christe, K. O.; Willner, H.; Sawodny, W. *Spectrochim. Acta, Part A* **1979**, *35A*, 1351.

(30) Kimura, K.; Bauer, S. H. *J. Chem. Phys.* **1963**, *39*, 3172.

(31) Tolles, W. M.; Gwinn, W. D. *J. Chem. Phys.* **1962**, *36*, 1119.

(32) Inoue, H.; Naruse, A.; Hirota, E. *Bull. Chem. Soc. Jpn.* **1976**, *49*, 1260.

(33) Oberhammer, H.; Boggs, J. E. *J. Mol. Struct.* **1979**, *56*, 107.

(34) Gundersen, G.; Hedberg, K. *J. Chem. Phys.* **1969**, *51*, 2500.

(35) Hencher, J. L.; Cruickshank, D. W. J.; Bauer, S. H. *J. Chem. Phys.* **1968**, *48*, 518.

(36) Christe, K. O.; Schack, C. J.; Curtis, E. C. *Spectrochim. Acta, Part A* **1977**, *33A*, 323.

(37) Shimanouchi, T. *Natl. Stand. Ref. Data Ser. (U.S. Natl. Bur. Stand.)* **1972**, *39*, 33.

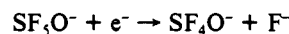
(38) McDowell, R. S.; Aldridge, J. P.; Holland, R. F. *J. Phys. Chem.* **1976**, *80*, 1203.

and INDO calculations, respectively, for the minimum energy structures, are insignificant and result in inversion energy barriers which are comparable to the zero-point energies of the inversion modes in the ground states.

A comparison between the observed (see Table I) and calculated (see Table II) *s*-orbital spin densities of SF₄⁻ shows qualitative agreement. Although the value of 0.033 calculated for the sulfur 3*s*-orbital spin density of the C_{4v} structure of SF₄⁻ is smaller than that of 0.103 derived from the observed ³³S hyperfine splitting, it should be noted that the former is very sensitive to small changes in the bond angle (see Table II). A slightly larger distortion of SF₄⁻ from D_{4h} symmetry could significantly increase the calculated 3*s*-orbital spin density on sulfur. In view of the relatively small energy difference between the C_{4v} and the D_{4h} structures (see above), the C_{4v} distortion and hence the hfs and spin densities could, in theory, be strongly temperature dependent. However, the experimental ³³S hyperfine splitting showed virtually no difference between 20 and 70 °C. Unfortunately, precise measurements at lower temperatures were precluded by anisotropic line broadening.

Comparison of SF₄⁻ with isoelectronic ClF₄ (see Table I) shows that SF₄⁻ has a slightly smaller *g*-factor than ClF₄, as expected from the smaller spin-orbit coupling of sulfur. Comparison of SF₄⁻ with SF₅¹² shows a marked difference (see Tables I-III). In SF₄⁻ the unpaired electron is concentrated mainly in the sulfur p_z orbital, whereas in SF₅ it is mainly located in an sp-hybrid orbital, which accounts for the much larger ³³S hfs of the latter.

SF₄O⁻ Radical Anion. By analogy to the generation of the SF₄⁻ radical anion by γ-irradiation of Cs⁺SF₅⁻ (see above), the novel SF₄O⁻ radical anion was generated by γ-irradiation of Cs⁺SF₅O⁻. In both cases, the probable reaction mechanism involves the loss of a fluorine ligand due to secondary electron capture.³⁹



The observed EPR spectrum exhibits hyperfine splittings due to four equivalent fluorine atoms, with weak satellite lines of 0.2% intensity due to the naturally occurring ³³S isotope. The fact that four equivalent fluorine atoms are present in the radical leaves no doubt that the observed radical is the *trans* isomer (III) rather than the *cis* isomer (IV). By analogy with *cis*-PF₄O²⁻ (see Table I), *cis*-SF₄O⁻ would be expected to exhibit three fluorine atoms, not necessarily equivalent, with large hfs and one fluorine atom with a very small hfs. As discussed above, the exclusive formation of the *trans*-SF₄O⁻ isomer is probably due to both energetic and reaction mechanistic reasons. If the fluorine atom were eliminated from the SF₅O⁻ precursor by random electron capture, the *cis* isomer would be four times more likely to form than the *trans* isomer.

As can be seen from Tables I and III, the orbital spin densities in isoelectronic *trans*-SF₄O⁻ and *trans*-PF₄O²⁻ are similar to those in SF₅ but deviate significantly from those in SF₄⁻. This indicates that in *trans*-SF₄O⁻ and SF₅ the unpaired electron is concentrated mainly in an axial sulfur sp-hybrid orbital, which accounts for their large ³³S hfs (see Table I). The experimentally found, high values of the 3*s*-orbital spin densities on sulfur in *trans*-SF₄O⁻ and SF₅ are also supported by the results from the LDF calculations (see Table III). However, the relatively large changes in the spin densities between isoelectronic *trans*-SF₄O⁻ and *trans*-PF₄O²⁻, predicted by the LDF calculations (see Table III), are not substantiated by the experimental data given in Table I. As indicated by the LDF calculations (see Table III), the axial oxygen or fluorine ligands in *trans*-SF₄O⁻ or SF₅ have little spin density, contrary to the case of *cis*-SF₄O⁻, for which the calculated total spin density on oxygen is 0.184 (see Table IV).

Bonding in SF₄⁻ and SF₄O⁻. For SF₄⁻, the LDF calculated and corrected (-0.04 Å) S-F bond length of about 1.75 Å suggests

(39) This mechanism has been demonstrated for electron capture by F₃NO and FClO₃, since their radical anions were observed by EPR to dissociate into F₂NO and ClO₃, respectively, on annealing to higher temperature. Nishikida, K.; Williams, F. *J. Am. Chem. Soc.* **1975**, *97*, 7166. Hasegawa, A.; Hudson, R. L.; Kikuchi, O.; Nishikida, K.; Williams, F. *J. Am. Chem. Soc.* **1981**, *103*, 3436. Hasegawa, A.; Williams, F. *J. Am. Chem. Soc.* **1981**, *103*, 7051.

long and weak bonds, when compared to normal S-F single bonds, which have values ranging from about 1.53 to 1.56 Å (see Table V). These long S-F bonds in SF₄⁻, combined with the above analysis of the electron spin density distribution, suggest the following idealized bonding scheme for SF₄⁻. The four equatorial fluorines are bound to sulfur by two semi-ionic, three-center-four-electron bond pairs⁴⁰⁻⁴³ involving the p_x and p_y orbitals of sulfur. The third p orbital of sulfur, the p_z orbital, accommodates primarily the unpaired free electron, while the remaining sulfur free valence electron pair is localized mainly in its s orbital.

For *trans*-SF₄O⁻, the bonding of the four equatorial fluorines (calculated bond length = 1.77 - 0.04 = 1.73 Å) is similar to that proposed above for SF₄⁻, i.e. weak, semi-ionic, three-center-four-electron bonds involving the sulfur p_x and p_y orbitals. The LDF calculated S-O bond length (1.464 - 0.04 = 1.42 Å) is comparable to normal S=O double bonds (*r*_{SO} in SF₄O = 1.406 Å),³⁴ supporting, for oxygen, a predominantly covalent bonding scheme through a sulfur sp₂ hybrid, which also accommodates, to a large extent, the unpaired free electron. The bonding scheme in SF₄O⁻ is completed by the formation of an additional double bond between sulfur and oxygen.

In SF₅, the basic bonding scheme somewhat resembles that in *trans*-SF₄O⁻, but the ionic character of the four equatorial bonds is less pronounced. This is not surprising in view of the lack of a formal negative charge (neutral radical versus radical anion) which strongly enhances semi-ionic bonding. This interpretation

is nicely supported by the atomic charges calculated by the LDF method for these radicals. As predicted from the above analysis, the negative charges on the four equatorial fluorine ligands decrease from -0.431 in SF₄⁻ to -0.376 in *trans*-SF₄O⁻ to -0.212 in SF₅.

Conclusions

The novel SF₄⁻ and *trans*-SF₄O⁻ radical anions⁴⁴ were prepared by γ-irradiation of SF₅⁻ and SF₅O⁻ containing salts, respectively, and were characterized by their isotropic EPR spectra, which permitted the determination of the s-orbital electron spin densities. Although anisotropic EPR data were not available for a complete electron spin density analysis, the nature and bonding of these interesting radical anions were elucidated using local density functional calculations. LDF theory was also used to predict the geometries and vibrational spectra of these and other closely related radicals. The reliability of these calculations was confirmed by comparison with experimental data from several well-known sulfur fluorides and oxyfluorides.

Acknowledgment. The work at Rocketdyne was financially supported by both the U.S. Army Research Office and the Air Force Phillips Laboratories. The work at the University of Tennessee was supported by the Division of Chemical Sciences, Office of Basic Energy Sciences, U.S. Department of Energy (Grant #DE-FG05-88ER13852).

(40) Pimentel, G. C. *J. Chem. Phys.* **1951**, *19*, 446.

(41) Hach, R. J.; Rundle, R. E. *J. Am. Chem. Soc.* **1951**, *73*, 4321.

(42) Rundle, R. E. *J. Am. Chem. Soc.* **1963**, *85*, 112.

(43) Wiebenga, E. H.; Havinga, E. E.; Boswijk, K. H. *Adv. Inorg. Chem. Radiochem.* **1961**, *3*, 158.

(44) Morton and Preston have noted in ref 6 that for isoelectronic pairs of radicals the F¹⁹ hyperfine interaction is always larger in the radical anion than in the neutral species. The results of the present study are in accord with this generalization, since the F¹⁹ splittings for SF₄⁻ and SF₄O⁻ are greater than those for ClF₄ and SF₅, respectively (see Table I).

Motional Processes in Solid Organotin Polymers Investigated by One- and Two-Dimensional ¹³C and ¹¹⁹Sn NMR Spectroscopy

Jörg Kümmerlen and Angelika Sebald*

Contribution from the Bayerisches Geoinstitut, Universität Bayreuth, Postfach 10 12 51, W-8580 Bayreuth, Germany. Received August 24, 1992

Abstract: Variable-temperature one- and two-dimensional ¹³C CP/MAS spectroscopy of a series of six crystalline trimethyltin compounds has demonstrated that the rate of Me₃Sn reorientation is significant on the NMR time scale. The combination of line shape analyses of the exchange-broadened ¹³C CP/MAS spectra with rates obtained from 2D exchange spectra yields activation energies in the range of 38.6–72.5 kJ mol⁻¹ for this series of compounds. Comparison of our NMR results with information from X-ray diffraction measurements leads us to postulate a 2π/3 propeller-like jump around the tin-oxygen or tin-nitrogen bond, respectively, as the reorientation mechanism. Rotor-synchronized ¹¹⁹Sn 2D magnetization-transfer experiments strongly support this view and indicate a rigid backbone for these chainlike polymers.

Introduction

Nuclear magnetic resonance (NMR) spectroscopy has proved to be a powerful tool for the elucidation of various types of molecular nonrigidity and fluxional behavior of organometallic complexes and molecules, both in solution and in the solid state.¹⁻³ Coherent averaging of anisotropic spin interactions by magic angle spinning (MAS), in combination with high power proton decou-

pling and cross-polarization (CP) techniques, enables the adoption of a variety of solution-state NMR techniques for the investigation of dynamic processes in solids, exploiting the properties of heteronuclei like ¹³C or others. In line with the development of high-resolution solid-state NMR spectroscopy, experimental methods for the investigation of such processes have become available, ranging from wide line and relaxation measurements on abundant nuclei to magnetization-transfer experiments in one, two, and three dimensions.^{4,5} This wide range of experimental

(1) Andrew, E. R.; Eades, R. G. *Proc. Roy. Soc. London* **1953**, *A218*, 537-552.

(2) Andrew, E. R. *J. Chem. Phys.* **1950**, *18*, 607-618.

(3) Sandström, J. *Dynamic NMR Spectroscopy*; Academic Press: London and New York, 1982.

(4) Blümich, B.; Spiess, H. W. *Angew. Chem.* **1988**, *100*, 1716-1734; *Angew. Chem., Int. Ed. Engl.* **1988**, *27*, 1655.

(5) Spiess, H. W. *Chem. Rev.* **1991**, *91*, 1321-1338.